

INFLUENCE OF TEMPERATURE ON NONLINEAR PIEZOELECTRICITY IN A PIEZOELECTRIC CERAMIC

Keisuke ISHII, Shinjiro TASHIRO and Kunihiro NAGATA

Department of Material Science and Engineering,
The National Defense Academy, 1-10-20, Hashirimizu, Yokosuka 239-8686, Japan
Fax +81-468-41-3810 ext 3353, e-mail: kishii@nda.ac.jp

In order to study the nonlinear piezoelectricity of a PZT piezoelectric ceramic vibrator at temperatures higher than room temperature, a nonlinear piezoelectric coefficient of 3rd higher term was measured at temperatures from room temperature to 120°C. The driving condition inducing a current-jumping phenomenon at the various temperatures was calculated using the nonlinear coefficient. The nonlinear coefficient became smaller with the increase of temperature, and the current-jumping phenomenon was suppressed at higher temperature regions.

Key words: piezoelectric ceramic vibrator, current-jumping phenomenon, nonlinear circuit equation, nonlinear piezoelectric coefficient, temperature dependence

1. INTRODUCTION

Using an effective nonlinear piezoelectric coefficient for a vibrator, ζ_{D31}' , we have estimated the unstable phenomena caused by the nonlinear piezoelectricity in piezoelectric ceramics driven at high power levels.[1-5] The ζ_{D31}' is a nonlinear piezoelectric coefficient of 3rd higher term for a PZT piezoelectric vibrator, measured in the high-power driving for a short time.[2] The analysis of the unstable phenomena using ζ_{D31}' is relatively insensitive to the surrounding conditions compared with the analysis using the linear material constants changing with sample temperature.[6,7] Hence, the analysis using ζ_{D31}' enables us to exactly estimate the instabilities even under various driving conditions. We have predicted the precise driving conditions inducing the nonlinear phenomena by the theoretical calculation with ζ_{D31}' . [4,5]

The dissolution of the solders bonding lead wires and the depolarization are often observed in the products of piezoelectric ceramics for the high-power driving, which results in serious troubles. This means that the driving temperature of piezoelectric devices exceeds 100°C in some cases. For designing practical piezoelectric devices used under the high-power driving, it is significant to quantitatively estimate the nonlinear piezoelectricity at such higher temperatures. However, the nonlinear piezoelectric coefficients at the higher temperatures have been hardly studied. In this report, ζ_{D31}' was measured for a piezoelectric vibrator at the temperatures from room temperature to 120°C using a thermostatic chamber. The current-jumping phenomena, which is a typical nonlinear phenomenon, were analyzed using measured ζ_{D31}' values, and the temperature dependence of driving condition inducing current-jump was examined.

2. EXPERIMENTAL

The sample configuration of a piezoelectric ceramic vibrator is a rectangular bar as shown in Fig. 1. A pair

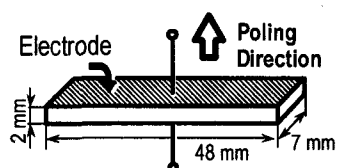


Fig. 1. Sample configuration.

of silver electrodes was fired on the upper and lower surfaces of the vibrator, the composition of which is $0.95\text{Pb}(\text{Zr}_{0.49}\text{Ti}_{0.51})\text{O}_3-0.05\text{Pb}(\text{Sb}_{0.5}\text{Nb}_{0.5})\text{O}_3-0.015\text{MnO}$. The sample was poled under an electric field of 3 kV/mm for 10 min in silicone oil bath kept at 120°C. The sample is “hard material” of $Q_m = 1700$. The motional impedance parameters and dumping capacitance at each temperature were measured at a small signal field using a gain phase analyzer (HP, 4194A).

All the measurements were performed in a thermostatic chamber (ESPEC, ST110B1). The ζ_{D31}' was measured in the sample driven at the fundamental resonance frequency of length extensional $1/2\lambda$ mode using a constant-current circuit illustrated in Fig. 2(a). To prevent sample heating due to the high-power driving, the sample voltage and current were simultaneously measured with a digital storage scope (Lecroy, LT344) at the moment after 20 ms from the application of an ac field. Using the Fourier-transform function in LT344, the magnitudes of the observable 3rd harmonic voltage and sample current were computed.

The current-jumping was observed with a constant-voltage circuit shown in Fig. 2(b). The voltage across the 5 Ω resistance was detected with an RF voltmeter (National, VP-8602A), and the analog-output voltage of VP-8602A was stored into LT344. Driving frequency was swept around the resonance frequency at a sweeping-time of 20 s for using a function generator of HP-3323B.

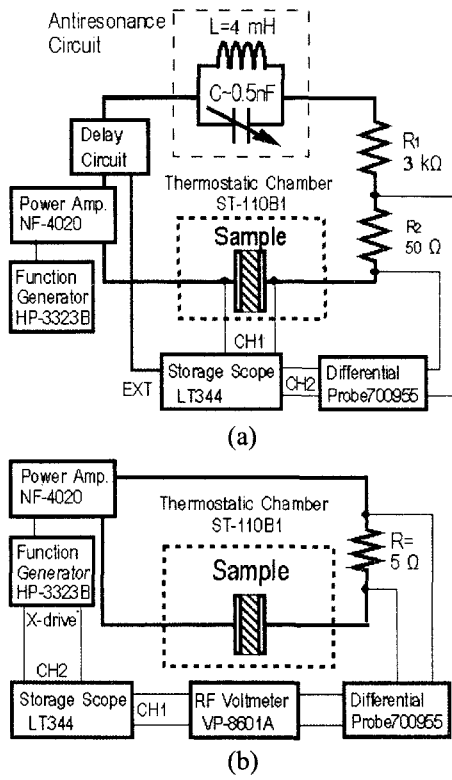


Fig. 2. Constant-current circuit for the measurement of nonlinear piezoelectric coefficient (a), and constant-voltage circuit for the measurement of current-jumping (b).

3. RESULTS AND DISCUSSION

The ξ_{D31}' indicates the relationship between the sample current, i_3 , and the 3rd nonlinear voltage generated in the sample, as shown in a nonlinear circuit equation, Eq. (1).[1-5]

$$v_3 = L \frac{di_3}{dt} + R i_3 + \frac{1}{C} \int i_3 dt + \gamma_{D31}' (\int i_3 dt)^2 + \xi_{D31}' (\int i_3 dt)^3 \quad (1)$$

The L , C and R are motional impedance parameters of the fundamental resonance, and γ_{D31}' is a nonlinear piezoelectric coefficient of 2nd higher term. When the sample is driven by a constant current $i_3 = I_0 \sin \omega t$, the instantaneous values of a fundamental voltage, v_0 , and a 3rd harmonic voltage, v_{h3} , obtained from Eq. (1) are expressed by Eqs. (2) and (3).

$$\begin{aligned} v_0 &= V_0 \sin(\omega t + \theta) \\ &= \left(\omega L - \frac{1}{\omega C} \right) I_0 \cos \omega t + R I_0 \sin \omega t - \frac{3\xi_{D31}'}{4\omega^3} I_0^3 \cos \omega t \\ &= \sqrt{\left\{ \left(\omega L - \frac{1}{\omega C} \right) I_0 - \frac{3\xi_{D31}'}{4\omega^3} I_0^3 \right\}^2 + (I_0 R)^2} \sin(\omega t + \theta) \\ \text{where, } \theta &= \tan^{-1} \left\{ \left(\omega L - \frac{1}{\omega C} - \frac{3\xi_{D31}'}{4\omega^3} I_0^2 \right) / R \right\} \end{aligned} \quad (2)$$

$$v_{h3} = V_{h3} \cos 3\omega t = \frac{\xi_{D31}'}{4\omega^3} I_0^3 \cos 3\omega t \quad (3)$$

Here, V_0 and V_{h3} are the amplitudes of the fundamental voltage and the 3rd harmonic voltage generated in the sample. In this report, ξ_{D31}' was calculated from V_{h3} in Eq. (3). Since the motional impedance at 3rd harmonic frequency, Z_{m3} , are relatively larger when the sample is driven at the fundamental resonance angular frequency, ω_r , the observable amplitude of V_{h3}' is considerably different from V_{h3} , as expressed by Eq. (4).[1,2]

$$V_{h3}' = \frac{Z_{C3}}{Z_{C3} + Z_{m3}} V_{h3} \quad \text{where, } Z_{m3} = R_3 + j \left(3L_3 \omega_r - \frac{1}{3C_3 \omega_r} \right) \quad (4)$$

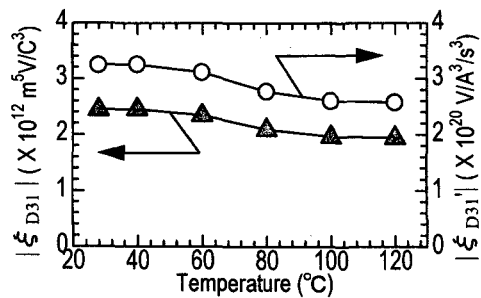
Here, L_3 , C_3 and R_3 are the motional impedance parameters of the 3rd resonance, and $Z_{C3} = 1/j3\omega_r C_3$ is the impedance due to the damping capacitance. Since the motion of the residual domain walls changes the elastic compliance of the material, the Z_{m3} changes with the increase of I_0 [2]. We need to obtain the variation of Z_{m3} corresponding to each current for calculation of the correct ξ_{D31}' values, but, it is difficult to exactly measure each Z_{m3} value. Assuming that the high-power driving changes only the C_3 value in the components of Z_{m3} (L_3 , C_3 , and R_3), the original values measured at low signal field with a 4194A can be converted the corresponding values to each current at each high-power level, as shown in Eq. (5) using ξ_{D31}' . [2]

$$C_3(I_0) = \frac{4\omega_r^2}{4\omega_r^2 + 3C_3 \xi_{D31}' I_0^2} C_3 \quad (5)$$

By substituting V_{h3} in Eq. (3) into Eq (4) which is obtained by replacing C_3 in Eq. (4) with $C_3(I_0)$, the quadratic equation of ξ_{D31}' is introduced as expressed in Eq. (6).[2]

$$\begin{aligned} & \frac{I_0^4}{16\omega_r^4} \left(\frac{9C_s^2 C_3^2 V_{h3}^{\prime 2}}{C_3^2} - \frac{I_0^2}{\omega_r^2} \right) \xi_{D31}'^2 \\ & + \frac{C_s C_3 I_0^2}{2C_3 \omega_r^2} \left(\frac{3C_s}{C_3} + 3 - 27C_s L_3 \omega_r^2 \right) V_{h3}^{\prime 2} \xi_{D31}' + \\ & \left(9R_3^2 C_s^2 \omega_r^2 + 1 + 81L_3^2 C_s^2 \omega_r^4 - 18L_3 C_s \omega_r^2 \right) V_{h3}^{\prime 2} = 0 \end{aligned} \quad (6)$$

The average of three ξ_{D31}' values obtained at the currents of 25, 30, and 35 mA using Eq. (6) was defined as a ξ_{D31}' value at each temperature. The intrinsic nonlinear coefficient as a material constant, ξ_{D31} , is calculated from ξ_{D31}' using Eq. (7).[1,8] The ξ_{D31} is a intrinsic material constant, which is independent of sample size and electrode configuration, even ξ_{D31}' is depend on them.


 Fig. 3. Temperature dependence of ξ_{D31}' and ξ_{D31} .

$$\xi_{D31}' = n \times \frac{d}{A^3} \xi_{D31} \quad (7)$$

Here, d and A are the thickness and the top surface area of the sample shown in Fig.1. The n is the conversion factor obtained by considering the electrode configuration, and is 2.284 in this study.[1,8]. Figure 3 shows the relationship between two nonlinear coefficients (ξ_{D31}' and ξ_{D31}) and sample temperature. The absolute values of ξ_{D31}' and ξ_{D31} decrease with the

increase of temperature, and they decreased down to 80 % of the room-temperature value at 120°C. Thus, the nonlinear piezoelectricity becomes smaller at higher temperatures.

The unstable phenomenon which is called “current-jumping” is often observed in piezoelectric vibrators driven by a constant voltage at around resonance frequency. The plots in Fig. 4 are the experimental spectra of the current-jumping phenomena at 40°C, 80°C, and 100°C. The applied voltages are 2V, 4V and 4V, respectively. The gray circles show amplitude of the sample current when the driving frequency increases from the lower frequency side, and white triangles show those when the driving frequency decreases from the higher frequency side. The solid and broken lines are the theoretical curves which are obtained by graphically solving I_0 - V_0 curves expressed by Eq. (2).[5] Although the theoretical curves are a little larger than the experimental values at higher temperatures, the theoretical curves represent the experimental frequency response of the current. This suggests that the analysis of the current-jumping phenomena using the nonlinear circuit equation of Eq. (2) is valid even at higher temperature region.

The calculation of the negative-resistance region in the I_0 - V_0 curve expressed by Eq. (2) gives us the driving

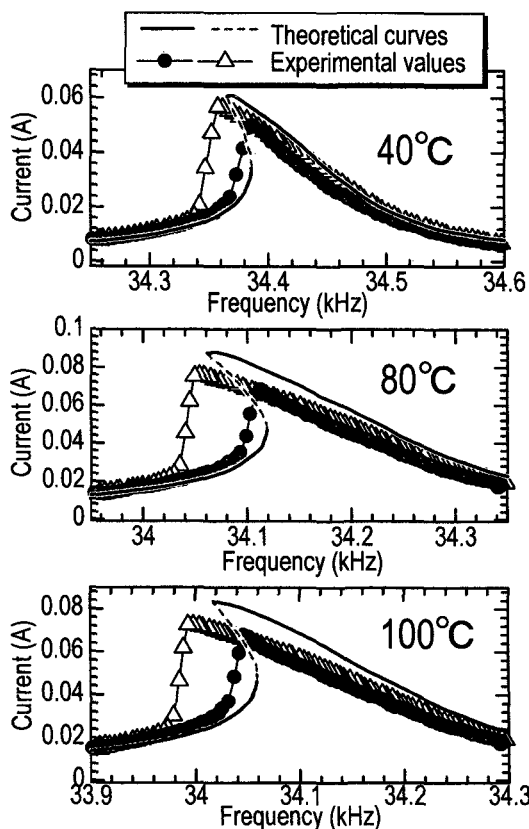


Fig. 4. Frequency spectra of current-jumping phenomena at each temperature. The gray circles and open triangles are measured values, and solid and broken lines are theoretical curves.

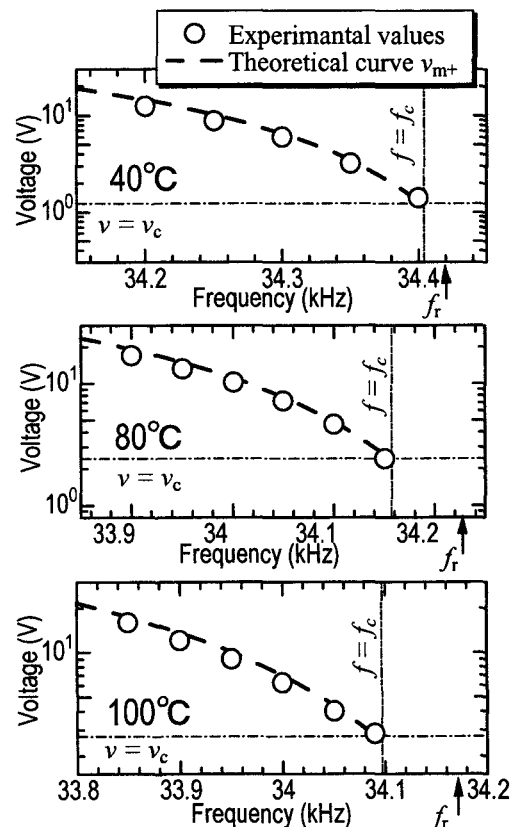


Fig. 5. Measured and calculated driving voltages inducing current-jumping when the driving frequency changed at the various temperatures. The open circles are measured values, and broken lines are theoretical curves calculated with Eq. (8).

condition inducing the current-jumping.[5] Equation (8) indicates the relationship between ω and the driving voltage, v_{m+} , inducing current-jumping when the driving voltage increases from low to high levels at a constant driving angular frequency ω . [5]

$$v_{m+} = \frac{4\omega^3}{9\xi_{D31}'} \left\{ 2(\omega L - 1/\omega C) + \sqrt{(\omega L - 1/\omega C)^2 - 3R^2} \right\} \times \sqrt{\frac{\xi_{D31}'}{2\omega^3} \left\{ (\omega L - 1/\omega C) - \sqrt{(\omega L - 1/\omega C)^2 - 3R^2} \right\}} \quad (8)$$

The broken lines in Fig. 5 show the theoretical curves of v_{m+} calculated from Eq. (8) at each temperature. The open circles illustrate the experimental values. The theoretical curves well represent the driving voltages inducing the current-jumping at each temperature. Furthermore, the driving areas inducing the current-jumping are calculated based on Eq. (8). Since v_{m+} needs to be real number for the actual appearance of the current-jumping, the critical frequency, f_c , which is the upper limit of driving frequency inducing the current-jumping, is expressed by Eq. (9).

$$f_c = \frac{-\sqrt{3RC} + \sqrt{3R^2C^2 + 4LC}}{4\pi LC} \quad (9)$$

The current-jumping never appear when the driving frequency exceeds f_c . The critical voltage, v_c , which is v_{m+} value at f_c , indicates the lowest voltage inducing the current-jumping in the piezoelectric ceramic. The v_c is expressed by Eq (10).

$$v_c = \frac{8\sqrt{6}\pi f_c R}{9} \sqrt{\frac{2\sqrt{3}R\pi f_c}{\xi_{D31}'}} \quad (10)$$

The solid and broken curves in Fig. 6 illustrate the theoretical values of v_c and f_r-f_c calculated from Eqs. (9) and (10). The f_c is lower than the resonance frequency, $f_r = \omega_r/2\pi = (CL)^{-1/2}/2\pi$. [5] Since the difference between f_r and f_c becomes larger with the increase of temperature, the possibility that the driving frequency enters the frequency region inducing the current-jumping decreases generally at frequencies around f_r . Besides this, the higher voltages must be applied for inducing the current-jumping at the higher temperatures because of the higher v_c . The experimental values shown as the plots in Fig. 6 are almost corresponding to these theoretical values. From these results, it was found

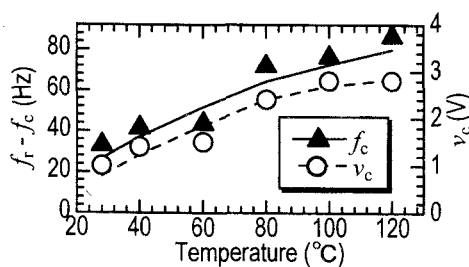


Fig. 6. Temperature dependence of v_c and f_r-f_c .

that the current-jumping becomes difficult to occur with temperature rise.

4. CONCLUSIONS

1. The nonlinear piezoelectric coefficient of 3rd higher term, which is measured from the 3rd harmonic voltages generated in a piezoelectric ceramic vibrator, becomes smaller with temperature rise.
2. With the increase of temperature, the critical voltage of the current-jumping increase, and the critical frequency becomes smaller compared with the resonance frequency. These results obtained from the theoretical calculation using the nonlinear coefficient well agree with the experimental results. They indicate that the increase of temperature suppresses the current-jumping.

REFERENCES

- [1] S. Tashiro, K. Ishii and K. Nagata, *J. Ceram. Soc. Japan.*, **110**, 649 (2002).
- [2] K. Ishii, S. Tashiro and K. Nagata, submitted in *J. Ceram. Soc. Japan.*
- [3] S. Tashiro, T. Murata, K. Ishii and H. Igarashi, *Jpn. J. Appl. Phys.*, **40**, 5679 (2001).
- [4] K. Ishii, T. Yamada, S. Tashiro, H. Igarashi, *Jpn. J. Appl. Phys.*, **38**, 5572 (1999).
- [5] K. Ishii, S. Tashiro and K. Nagata, *Trans. Mater. Res. Soc. of Japan*, **27**, 265 (2002).
- [6] M. Umeda, K. Nakamura and S. Ueha, *Jpn. J. Appl. Phys.*, **38**, 5581 (2000).
- [7] R. Herbit, U. Robelts, H. Dederichs and G. Arlt, *Ferroelectrics*, **98**, 107 (1989).
- [8] K. Ishii, S. Tashiro, K. Nagata, *Jpn. J. Appl. Phys.*, **41**, 7095 (2002).

(Received December 21, 2002; Accepted January 31, 2003)